Neurochem Res
DOI 10.1007/s11064-006-9165-0

ORIGINAL PAPER

The Neurotoxic Effect of Cuprizone on Oligodendrocytes Depends on the Presence of Pro-inflammatory Cytokines Secreted by Microglia

L. A. Pasquini · C. A. Calatayud · A. L. Bertone Uña · V. Millet · J. M. Pasquini · E. F. Soto

Accepted: 6 September 2006

Abstract In order to further characterize the still unknown mechanism of cuprizone-induced demyelination, we investigated its effect on rat primary oligodendroglial cell cultures. Cell viability was not significantly affected by this treatment. However, when concentrations of IFNγ and/or TNFα having no deleterious effects per se on cell viability were added together with cuprizone, cell viability decreased significantly. In mitochondria isolated from cuprizone-treated glial cells, we observed a marked decrease in the activities of the various complexes of the respiratory chain, indicating a disruption of mitochondrial function. An enhancement in oxidant production was also observed in cuprizone and/or TNFα-treated oligodendroglial cells. In in vivo experiments, inhibition of microglial activation with minocycline prevented cuprizone-induced demyelination. Based on the above-mentioned results we suggest that these microglial cells appear to have a very active role in cuprizone-induced oligodendroglial cell death and demyelination, through the production and secretion of pro-inflammatory cytokines.

Keywords Cuprizone · Cytokines · Oligodendrocytes · Myelin · Demyelination · Microglia

This work is dedicated with sincere friendship to Celia and Tony Campagnoni.

L. A. Pasquini · C. A. Calatayud · A. L. Bertone Uña · V. Millet · J. M. Pasquini · E. F. Soto (✉)
Departamento de Química Biológica, Facultad de Farmacia y Bioquímica, Universidad de Buenos Aires, Junin 956, Buenos Aires C1113AAD, Argentina
e-mail: edufsoto@mail.retina.ar

Introduction

The effects of Bis-(cyclohexanone)-oxaldihydrazone (cuprizone, CPZ) on weanling rodents provide a protocol for toxic demyelination in which degeneration of oligodendrocytes precedes disruption of the myelin sheath. Samples taken from rodent brains during the time-course of CPZ intoxication exhibit ultrastructural signs of oligodendrocyte degeneration, prior to the vacuolation of oligodendrocytes and myelin sheaths [1, 2], and declines in the mRNAs of myelin proteins [3]. Investigators from at least three laboratories observed enlargement of mitochondria in oligodendrocytes in the brains of CPZ-treated rodents [4–6]. In these animals, copper, which is an essential component of the mitochondrial enzyme cytochrome oxidase, was found to be around 50% of normal and the reaction rate of cytochrome oxidase around 77% of normal [7, 8].

The administration of CPZ also produces a rapid proliferation and accumulation of microglia/macrophages in the corpus callosum, one of the main targets of CPZ, previous to demyelination [9]. TNFα is a multipotent pro-inflammatory cytokine. Acting through TNFR1 it is believed to mediate cell death while when its action is exerted through TNFR2, it is known to enhance cell death or cell growth and proliferation, depending on the type of cell. In the CNS, microglia and astrocytes are the main producers of TNFα. Conflicting results have indicated either an exacerbating or an ameliorating role of TNFα during experimentally induced brain trauma [10] and in a murine model of multiple sclerosis [11, 12].

Inflammation and an increase in the levels of TNFα and IFNγ induces apoptosis in a dose-dependent

manner in two human oligodendroglial cell (OLGc) lines such as HOG and MO3.13 and it has been shown that their effects on cell death are synergistic [13]. In vitro studies have demonstrated a cytotoxic role for TNFα on oligodendrocytes [14, 15].

Cammer [16] showed that CPZ treatment of oligodendrocyte-enriched glial cell cultures or of mixed glial cell cultures from neonatal rat brains for 1 h, inhibited the maturation of oligodendrocytes and appeared to affect their mitochondria, without diminishing the number of precursors. As far as we know, this is the only work in which the direct effect of CPZ on OLGc cultures has been investigated and it should be stressed that in spite of the many studies related to the deleterious effects of CPZ on OLGcs, we are still quite far from knowing which are the mechanisms involved in its action.

In the present study we investigated the effects of CPZ added to rat primary OLGc cultures. We found that the mechanism through which CPZ induces demyelination does not seem to be due to a direct action of the neurotoxic on the myelin-forming cells. On the other hand, addition of CPZ to these cultures together with TNFα and/or IFNγ produced a marked increase in cell death. These results suggest that CPZ-induced myelin damage appears to be mediated by certain molecules such as TNFα and IFNγ which are secreted by the surrounding cells: microglia/macrophages. We also observed that CPZ treatment induces a diminished activity of mitochondrial complexes in OLGcs, with the consequent decrease in energy production and an increase in the output of oxidants. Based on these data, we hypothesize that the mechanism through which CPZ induces demyelination could be due to a decrease in energy production by OLGc mitochondria and an increase in the production of oxidants, leading to the recruitment of microglia/macrophages, which through the secretion of high levels of inflammatory cytokines could finally induce OLGc death. The experiments in which we investigated the neuroprotective effect of minocycline on mice submitted to CPZ-induced demyelination give strong support to our predictions.

Experimental procedure

Materials

All chemicals used were of analytical grade and were obtained from Sigma Chem. Co. (St Louis, MO). Dulbecco's modified Eagle's medium, Ham's F12 (DMEM/F12) and Hank's solution was from Hyclone (Logan, UT). Bovine insulin, progesterone, putrescine, sodium selenite, T3, penicillin, streptomycin, poly-L-lysine, transferrin, trypsin, MTT (3-(4,5-Dimethylthiazol-2-yl)-2,5-diphenyl-tetrazolium bromide), CPZ, Ac-DEVD-AMC, Ac-DEVD-CHO, Hoechst 33342, 2,3-dimethoxy-6-methyl-1,4-benzoquinone, rotenone, cytochrome *c*, NADH, succinate, propidium iodine and minocycline were obtained from Sigma (St. Louis, MO). Anti-MBP antibody was a generous gift from Dr. Anthony Campagnoni (Mental Retardation Research Center, University of California at Los Angeles). Anti-CD11b was obtained from Chemicon Int. (Temecula, CA) and anti-NFκB (p65 subunit) was purchased from Santa Cruz Biotechnology Inc. (Santa Cruz, CA). Cycletest^{TM} Plus DNA Reagent Kit was from Pharmingen-Becton Dickinson, Co (San Diego, CA). BrainStain Imaging Kit and 5(or 6)-carboxy-2′7′-dichlorodihydroxyfluorescein diacetate (DCDCDHF) were obtained from Molecular Probes (Eugene, OR). Fluorsave was from Calbiochem (La Jolla, CA).

Animals

Newborn Wistar rats were used to obtain cell cultures for in vitro studies (see below). For in vivo experiments, eight-week-old male Swiss mice, weighing around 30 g were used throughout. In both cases, animals were housed in groups of four animals under controlled temperature (22 ± 2°C) in an artificially lit animal room under a 12-h cycle period and fed with water and food ad libitum.

Oligodendroglial cell cultures

Primary cultures of OLGcs were performed basically as described by McCarthy and de Vellis [17]. Cerebral hemispheres were dissected out from newborn rats, freed of meninges, and dissociated by gentle repetitive pipetting in a mixture of DMEM and Ham's F12 (1:1 v/v) containing 5 μg/ml streptomycin and 5 U/ml penicillin, supplemented with 10% fetal calf serum (FCS). The cell suspensions were seeded in poly-L-lysine-coated 75-cm^2 tissue culture flasks. After 14 days in culture, microglia was separated by shaking the flasks for 30 min in an orbital shaker at 150 rpm/min and OLGcs were separated from astrocytes by continuous shaking for 24 h at 240 rpm/min. The cell suspension obtained was filtered through a 15-μm mesh filter and then centrifuged at 1,500 rpm for 10 min. Oligodendrocyte progenitors were grown for 48 h in a medium containing 1/3 B104 conditioned medium and 2/3 of

unconditioned glial defined medium (GDM: DMEM/F12 supplemented with glucose 4 g/l, $NaHCO_3$ 2.4 g/l, insulin 25 mg/l, putrescin 8 mg/l, transferrin 50 mg/l, T3 9.8 μg/l, progesterone 20 nM, sodium selenite 8 μg/l, and biotin 10 μg/l) [18] plus 0.5% FBS and plated on poly-L-lysine-coated Petri dishes (2×10^6 cells per dish) for biochemical studies or on poly-L-lysine-coated coverslips placed in multiwell plates (25×10^3 cells per well) for morphological and immunocytochemical studies. Cell cultures, evaluated quantitatively with O4, anti-neurofilaments and anti-GFAP antibodies were 95% pure.

Astrocyte cultures

Astrocytes were also prepared from newborn rat cerebral tissue as described by McCarthy and De Vellis [17]. Cerebral hemispheres were dissected out and processed as described above. After 14 days in culture, astrocytes were separated from microglia and oligodendrocytes by continuous shaking at 240 rpm/min during 24 h, in an orbital shaker. To ensure the complete removal of all oligodendrocytes and microglia, shaking was repeated once more after 1 or 2 days. Attached cells were trypsinized (1% trypsin in Hank's solution for 10 min), and after neutralizing with FCS, the cells were suspended in GDM [18] and distributed into Petri dishes for biochemical studies, or on poly-L-lysine-coated round coverslips placed in multiwell plates, for morphological and inmunocytochemical studies. The cells, that were around 95% pure, were kept in GDM for 24 h before treatment. Flat, round polygonal and elongated cells that were GFAP positive were identified as astrocytes.

Cell viability

The MTT survival assay was performed as described by Mosmann [19]. MTT was dissolved in PBS (5 mg/ml) and sterilized by passage through a Millipore filter (0.22 μm). This solution was added to the wells containing cultured cells, and the microplate was incubated at 37°C for 45 min. Viable cells with active mitochondria cleave the tetrazolium ring into a visible dark blue formazan reaction product. After the addition of SDS (5% final concentration in 0.05 M HCl per well) to stop the reaction, the product was quantified by spectrophotometry at 570 nm (six samples for each experimental condition). Since CPZ absorbs light at this wavelength, we corrected the values obtained by subtraction of the absorbance of CPZ at the concentration present in the sample.

Assay of caspase-3 activity

Caspase-3 activity was determined in lysates of cultured cells using the assay which depends on the cleavage of a fluorogenic synthetic tetrapeptide, Ac-DEVD-AMC specific for caspases. The levels of relative fluorescence of the liberated product (AMC) were measured on a Kontron spectrofluorometer, using a $\lambda_{excitation}$ of 380 nm and a $\lambda_{emission}$ of 430 nm. The blocking reaction was carried out adding the specific caspase-3 inhibitor Ac-DEVD-CHO. Results were normalized against the protein concentration of the cell lysate.

Immunocytochemistry

Cultured OLGcs were fixed for 2 h in 4% paraformaldehyde (PFA) in PBS at room temperature and then treated with 1% glycine in PBS for 15 min. When permeabilized OLGcs were used, they were incubated in 0.1% Triton X-100 in PBS for 15 min. Samples were blocked with 1% BSA in PBS for 2 h at 37°C and incubated overnight at 4°C with the primary antibody anti-NFκB (p65 subunit) (1/100). The coverslips were rinsed and incubated with anti-rabbit (1/500) fluorescent antibody. After immunostaining, nuclei were stained with the fluorescent dye Hoechst 33342 (5 μg/ml in 1% DMSO) [20]. The cell preparation was washed, mounted in Fluorsave, and analyzed by UV light microscopy. Microscopic observations were done by epifluorescence with an Olympus BX50 microscope.

Quantitative analysis of the cell cycle by flow cytometry

Control and treated OLGcs were harvested in their culture medium, pelleted by centrifugation at 500*g* for 5 min, rinsed with PBS, and used for the quantitative analysis of the different stages of the cell cycle using the Cycletest™ Plus DNA Reagent Kit mentioned above, as instructed by the manufacturers. Flow cytometry was carried out using the Mod Fit LT cell cycle analysis software (Verity Software, Topsham, ME).

Isolation of mitochondria from glial cell cultures

Confluent mixed glial cell cultures from 75-cm^2 flasks were used for this purpose. Cells were harvested using 0.25% trypsin, with cells from at least six flasks pooled to generate a single sample. Cells from at least three separate preparations obtained on different days were

utilized to generate data in the present report. Following the addition of trypsin, the cells were pelleted by centrifugation at 300*g* for 5 min at 4°C. All the subsequent steps were performed on ice or at 4°C. The mitochondrial fraction was obtained by differential and gradient centrifugation of the cellular pellet, as described by De Robertis et al. [21] and assay of different mitochondrial activities were done immediately following their isolation.

Activity of mitochondrial complexes

The activities of mitochondrial complexes were evaluated on the purified mitochondrial fraction obtained as described above. Complex I activity was measured determining the decrease in NADH absorbance at 340 nm, which leads to the reduction of benzoquinone. The activity was determined using the rotenone sensitive rate. Complex I–III was determined measuring the increase in absorbance at 550 nm by the reduction of cytochrome *c* using NADH as substrate. Complex II–III was measured using succinate as substrate by the reduction of cytochrome *c* at 550 nm [22].

Determination of oxidants

The level of oxidants was evaluated using the probe DCDCDHF. This probe interacts with oxidant species and can be visualized by its fluorescence. Cells submitted to the different treatments were preincubated with DMEM containing 50 μM of DCDCDHF. After 30 min at 37°C, cells were washed with PBS and then incubated in PBS containing 0.1% Igepal. After 30 min incubation with regular shaking, the fluorescence was measured at 525 nm ($\lambda_{excitation}$ 475 nm). Determination of DNA content was done adding to the sample 50 μM propidium iodine. Fluorescence was determined at $\lambda_{excitation}$ 538 nm; $\lambda_{emission}$ 590 nm. Results are expressed as percentage relative to control, of the fluorescence ratio between DCDCDHF/propidium iodine.

In vivo experiments

To induce demyelination, mice were fed a diet containing 0.2% (w/w) CPZ for 3–6 weeks, following the procedure previously described by Matsushima and Morell [23]. Age-matched control animals were maintained on the same diet without CPZ. At the end of CPZ treatment, animals were used for further studies.

A group of mice was used to evaluate the effects of minocycline on CPZ-induced demyelination. After one week under CPZ treatment, intoxicated mice were intraperitoneally injected with minocycline, according to the following protocol: 50 mg/kg, twice daily for the first two days, then 50 mg/kg once daily the next five days, and 25 mg/kg per day thereafter [24]. Animals were killed at 5 weeks of CPZ feeding and minocycline treatment and used for histological and immunohistochemical studies.

Another group of animals was used to analyze mitochondrial activities as described above. For these experiments, mice were fed CPZ for 3 or 6 weeks. Total brain homogenates obtained from these animals were used to isolate the purified mitochondrial fraction by differential and gradient centrifugation as described by De Robertis et al. [21].

Preparation of the tissues and microscopic examination

For microscopic observations, we used 4–6 animals per group. Animals were anesthetized with ethyl ether and perfused through the left ventricle of the heart with 30 ml of PBS followed by a 4% solution of PFA in PBS. The brains were carefully dissected out and post-fixed in the same solution overnight, followed by thorough washing in PBS and cryoprotection in 15% and 30% sucrose in PBS for 24 h. The tissue was then frozen and used to obtain 20 μm cryostat coronal sections using a Leica CM 1850 cryotome. The sections obtained from different areas of the brain and from the various experimental groups were mounted onto gelatin-precoated glass slides.

Microscopic observation was done by light microscopy or by epifluorescence using an Olympus BX50 microscope. Photography was carried out with a CoolSnap digital camera and the Image Pro Plus software (version 5.5) was used for image analysis.

Immunohistochemistry

For immunohistochemistry, cryotome sections were rinsed twice with PBS (pH 7.4) followed by PBS 0.025% Triton X100 (only for cytosolic antigens) and then blocked overnight with a solution containing 3% BSA plus 2% FCS in PBS. Incubation with the primary antibodies was done overnight at 4°C. The primary antibodies used were anti-MBP (1/100) and anti-CD11b (1/100). The sections were then incubated with a fluorescent-conjugated anti-rabbit or anti-mouse secondary antibody (Cy2) for 90 min at 37°C. Preparations were mounted in Fluorosave and examination was done as mentioned above.

Myelin staining

Two different procedures were used to stain myelin in cryosections: Sudan Black and a fluorescent staining procedure. For Sudan Black staining, sections were post-fixed for 5 min in 70% ethanol before immersion in a solution of Sudan black in 70% ethanol for 30 min. Excess stain was removed by washing with 70% ethanol. Preparations were mounted and examination was done as mentioned above. For the fluorescent staining we used the BrainStain Imaging Kit recently developed by Molecular Probes which uses FluorMyelin Green to selectively label myelin, DAPI to stain nuclei and Neurotrace 530/615 to stain neuron cell bodies (Nissl substance). Since for our purposes, staining of neurons was unnecessary, we only used the first two dyes as suggested by the manufacturers. The kit was used according to their instructions. The stained sections were mounted in Fluorsave and examination was done as mentioned above.

Statistical analysis

The Student *t*-test was used for the statistical analysis. A $P < 0.05$ was considered statistically significant. Data are given as means ± SEM.

Results

Figure 1A shows that after 24–72 h of treatment with concentrations of CPZ up to 1,000 μM, viability of OLGcs in culture was not significantly affected in comparison to controls. In order to find out if astrocytes had any role or influence in the OLGc death observed in in vivo CPZ intoxication, experiments were done in which astrocyte cultures were first treated with different concentrations of CPZ for 24 h. The supernatant obtained from these cultures was then used to treat OLGcs cultures. The assay was done in the presence or absence of 1,000 μM CPZ. Figure 1B shows that no changes in cell viability were observed under these conditions.

Since as mentioned before, CPZ treatment in vivo produces a rapid proliferation and accumulation of microglia/macrophages in the affected areas, cells which are known to produce cytokines, we decided to investigate if CPZ-induced myelin damage was ultimately mediated by certain molecules such as TNFα and IFNγ which are secreted by the surrounding cells. When these cytokines were added to OLGc cultures for 72 h at concentrations between 0 ng/ml and 50 ng/ml, which according to our preliminary studies do not affect cellular viability significantly, together with 1,000 μM CPZ, there was a significant decrease in cell viability (Fig. 1C).

In order to evaluate the proliferative state of the OLGcs, the cell cycle of cells treated with either CPZ and/or inflammatory cytokines was analyzed by flow cytometry. In the presence of IFNγ and/or TNFα or in the presence of CPZ alone, there was a 35% increase in the percentage of cells in the S phase, which was greater when the culture was carried out in the presence of the cytokines plus CPZ (46%) (Table 1).

Since several mitochondrial alterations have been described during CPZ intoxication, we decided to explore the activities of complex I, I–III and II–III of the mitochondrial respiratory chain in mitochondria isolated from brains of mice submitted to CPZ intoxication for different times as well as in mitochondria isolated from glial cell cultures previously treated with 1,000 μM CPZ during 72 h. The results show that in the mitochondria isolated from brains of mice submitted to CPZ intoxication for 3 and 6 weeks, there was a significant decrease in the activities of Complex I plus III (Fig. 2A) and Complex II plus III (Fig. 2B) of the respiratory chain. Similar results were obtained in the activities of Complex I (Fig. 2C) and Complex I plus III (Fig. 2D) of the respiratory chain in mitochondria isolated from glial cell cultures treated for 72 h with 1,000 μM CPZ.

Production of oxidants was evaluated using the probe DCDCDHF. This probe crosses the membrane and after oxidation is converted into a fluorescent compound. In cells treated with TNFα or CPZ alone, there was a significant increase in oxidants relative to controls. In the presence of both TNFα and CPZ the increase was much higher. On the contrary, when IFNγ was assayed alone or together with CPZ, the production of oxidants was similar to controls (Fig. 3).

Mitochondrial-derived reactive oxygen species (ROS) have been proposed to be instrumental in initiating apoptosis. Increased ROS production causes lipid peroxidation in mitochondrial membranes and triggers these organelles to release caspase-activating proteins such as cytochrome *c*. In order to evaluate whether this phenomenon was induced in OLGcs treated with CPZ plus TNFα and/or IFNγ and taking into consideration that several apoptotic pathways converge in the activation of caspases, we evaluated the activity of caspase-3 in treated OLGc cultures. Our results show a significant activation of this enzyme in cells treated with CPZ plus TNFα and/or IFNγ, suggesting that cell death in our experimental design is induced by a caspase-dependent pathway (Fig. 4).

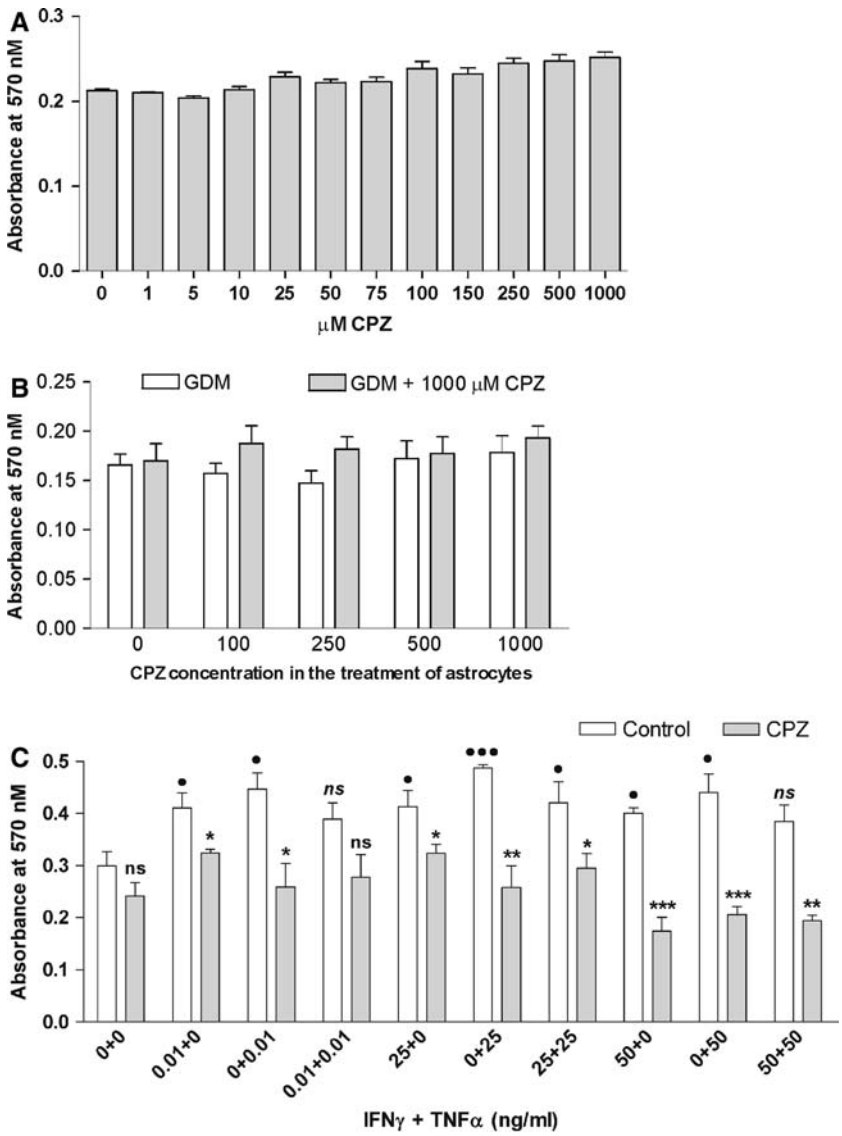

Fig. 1 **(A)** Effect of different concentrations of CPZ on OLGc viability. OLGcs were incubated in serum-free GDM for 2 h, then treated with different concentrations of CPZ for 72 h. Cell viability was determined by the MTT assay as described in Experimental Procedure. Values are the means ± SEM of three independent experiments (six replicates per experiment). Statistical differences were nonsignificant. **(B)** OLGc viability in cultures treated with astrocyte-conditioned media. Cultured astrocytes were treated with different concentrations (0–1,000 μM) of CPZ. The supernatant obtained from these cultures (conditioned media) was used to treat cultured OLGcs during 72 h. The assay was done in the presence (gray bars) and absence (white bars) of 1,000 μM CPZ. Cell viability was determined by the MTT assay as described in Experimental Procedure. Values are the means ± SEM of three independent experiments (six replicates per experiment). Statistical differences were nonsignificant. **(C)** Effect of different concentrations of TNFα and/or IFNγ in the presence or absence of CPZ on OLGc viability. OLGcs were incubated for 72 h with different concentrations of cytokines in the presence (gray bars) or absence (white bars) of 1,000μM CPZ. Cell viability was determined by the MTT assay as described in Experimental Procedure. Values are the means ± SEM of three independent experiments (six replicates per experiment). Statistical differences: $^{*}P < 0.05$, $^{**}P < 0.01$, $^{***}P < 0.001$ relative to control plus cytokine. ns: nonsignificant. $^{\bullet}P < 0.05$, $^{\bullet\bullet\bullet}P < 0.001$ relative to control without CPZ or cytokine

TNFR1 signals, which are predominantly expressed by OLGcs, induce both an apoptotic cascade and a protective NFκB-dependent cascade, whereas TNFR2 signals, expressed together with TNFR1 by microglia, primarily induce the protective NFκB cascade. We evaluated the expression of NFκB and its localization in controls, CPZ, TNFα, and CPZ plus TNFα-treated OLGc cultures by immunocytochemistry (Fig. 5). A strong positive immunostaining was observed in OLGcs exposed to CPZ or TNFα alone, but in

Table 1 Analysis of the cell cycle in OLGcs treated with CPZ and/or TNFα and/or IFNγ

Sample	Go–G1	G2–M	S	*P* value	G2–G1
GDM	89.7 ± 4.3	4.11 ± 1.5	6.2 ± 0.6	–	2.00
CPZ	87.9 ± 4.6	3.52 ± 0.9	8.6 ± 1.3	0.0440	2.02
IFNγ	88.8 ± 5.1	3.18 ± 1.1	8.0 ± 0.90	0.0449	2.01
TNFα	87.2 ± 6.1	4.12 ± 0.8	8.7 ± 1.0	0.0206	2.02
TNFα + IFNγ	88.3 ± 4.2	3.88 ± 0.9	7.8 ± 0.7	0.0397	2.00
CPZ + IFNγ	86.9 ± 6.2	3.77 ± 1.2	9.3 ± 0.9	0.0077	2.01
CPZ + TNFα	87.2 ± 3.2	4.15 ± 1.3	8.6 ± 0.9	0.0184	2.01
CPZ + TNFα + IFNγ	87.5 ± 6.4	3.23 ± 1.0	9.2 ± 1.1	0.0143	2.01

The cell cycle of OLGcs treated for 24 h with either CPZ (1,000 μM) and/or TNFα (50 ng/ml) and/or IFNγ (50 ng/ml) was evaluated by flow cytometry. Results are expressed as percentage of cells in the different phases of the cell cycle. Values are the means ± SEM of three independent experiments. Statistical differences in the S phase were evaluated relative to GDM (control). $P < 0.05$ was considered statistically significant

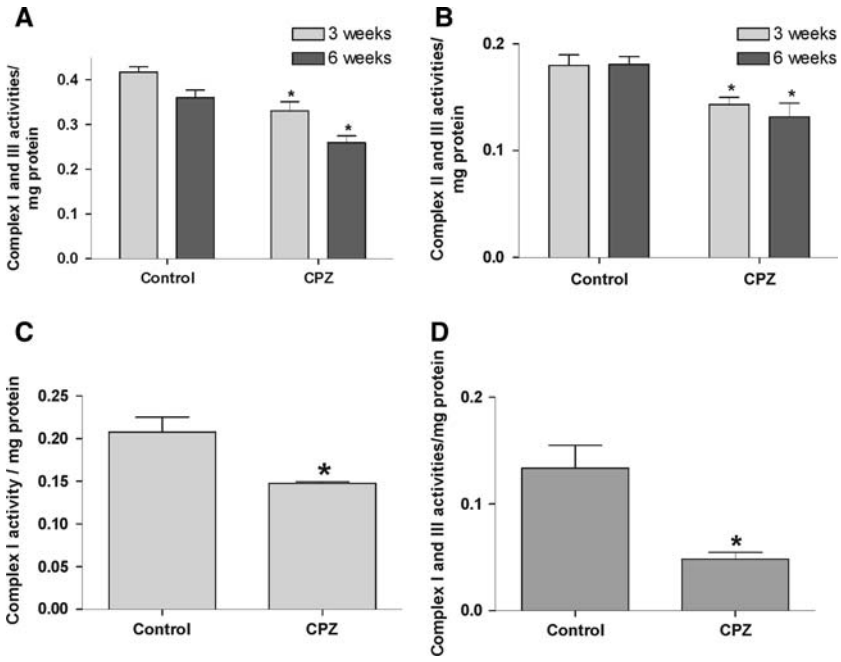

Fig. 2 Activities of Complex I–III **(A)** and II–III **(B)** of the respiratory chain evaluated in mitochondria isolated from total brain homogenates obtained from mice fed with CPZ for 3 or 6 weeks and controls. Values are the means ± SEM of three independent experiments (three replicates per experiment). Statistical differences: $*P < 0.05$. Activities of Complex I **(C)** and I–III **(D)** of the respiratory chain evaluated in mitochondria isolated from glial cultures treated with 1,000 μM CPZ during 72 h. Values are the means ± SEM of three independent experiments (three replicates per experiment). Statistical differences: $*P < 0.05$

comparison with the staining observed in the control cells, the strongest immunostaining was detected when the cells were incubated in the presence of both CPZ plus TNFα. In these situations, we observed that there was translocation of NFκB to the nucleus in a percentage of cells, suggesting that there was an activation of this factor.

With reference to the in vivo experiments, we found that in mice intoxicated with CPZ that were treated with minocycline, demyelination of the corpus callosum evaluated by Sudan Black (Fig. 6), fluorescent staining with the BrainStain Imaging Kit (Fig. 7), and by MBP immunostaining (Fig. 8), was much less than in the untreated controls. To investigate the mechanisms involved in the protective effects of minocycline, we examined microglial activation by inmunostaining with CD11b (MRC OX42) which recognizes both resting and activated microglia. We found that the number of CD11b positive cells was much smaller in the treated animals than in their respective controls, suggesting that this antibiotic is inhibiting microglial activation (Fig. 9).

Discussion

It is well known that feeding young adult mice with CPZ for a few weeks produces a massive demyelination in certain areas of the brain, particularly in the corpus callosum [4, 6, 23]. In the present study we carried out two different types of experiments in order to further characterize the mechanisms through which CPZ induces OLGc damage and demyelination. For the in vivo experiments, in which we analyzed the

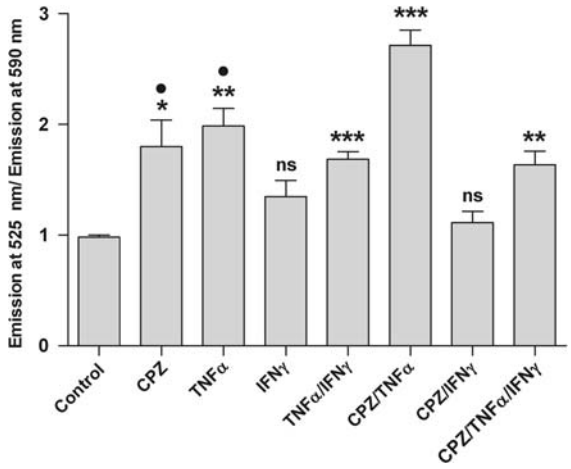

Fig. 3 Production of oxidants in OLGcs treated with CPZ (1,000 μM) or TNFα (50 ng/ml) or IFNγ (50 ng/ml) for 72 h. The fluorescent probe DCDCDHF was used to evaluate oxidants. Values are the means ± SEM of three independent experiments (eight replicates per experiment). Statistical differences: $^{*}P < 0.05$, $^{**}P < 0.01$, $^{***}P < 0.001$ relative to control. ns: nonsignificant. $^{\bullet}P < 0.05$ relative to CPZ (1,000 μM) plus TNFα (50 ng/ml)

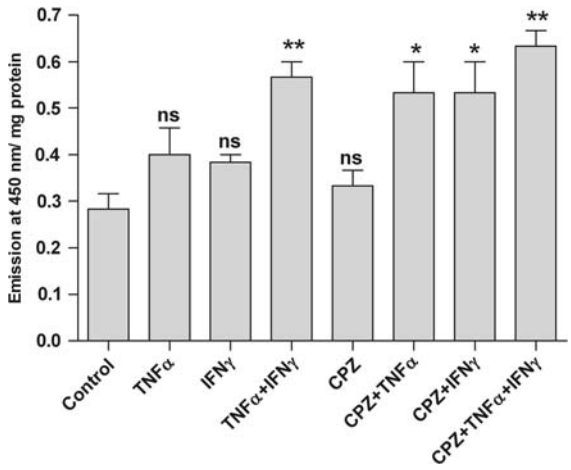

Fig. 4 Determination of caspase-3 activity on OLGcs treated with CPZ (1,000 μM) or TNFα (50 ng/ml) or IFNγ (50 ng/ml) for 72 h. Values are the means ± SEM of three independent experiments (three replicates per experiment). Statistical differences: $^{*}P < 0.05$, $^{**}P < 0.01$ relative to control. ns: nonsignificant

effects of CPZ intoxication on isolated brain mitochondria as well as the effect of treatment with minocycline on the prevention of CPZ-induced demyelination, we used young adult mice fed CPZ as described by Matsushima and Morell [23]. In the second set of experiments, in which we analyzed the in vitro effects of CPZ on OLGc primary cultures, we used rat brains, since mouse brains are well known to give a very low yield of OLGcs in culture, making it necessary to use a large number of animals in order to obtain reasonable amounts of material. Within this context it should be mentioned that although several studies indicated that the demyelination produced by CPZ is only observed in mice, we have recently shown that feeding 21-day-old Wistar rats with a diet containing 0.6% CPZ is effective in producing clear biochemical and histological evidences of demyelination [25], similar to those described in mice.

In spite of the many studies related to the effects of CPZ, the mechanism(s) through which this drug induces demyelination are not well known. CPZ is known to act as a copper chelator and it has been assumed, although not proven, that in the animals fed with this toxic, binding of copper, which results in copper deficiency, is responsible for demyelination. It is interesting to point out that damage to other cells in the CNS is not observed.

As far as we know, the only study related to the in vitro effect of CPZ was done by Cammer [16] who showed that CPZ treatment of OLGc-enriched glial cell cultures or mixed glial cell cultures from neonatal rat brains induced morphological evidences of damage to OLGc mitochondria and inhibited maturation of the precursor OLGcs present in the culture.

Regarding the effects of CPZ on OLGc cultures, it was surprising to find out that in spite of the high doses of CPZ added to the OLGc cultures (up to 1,000 μM) and the long incubation time (up to 72 h), their viability was quite similar to that of untreated controls. Although one possible explanation for these negative results could be that in these experiments, the action of CPZ was not sustained for long periods, as occurs in the in vivo studies, they prompted us to investigate whether OLGc damage produced by CPZ when used in vivo, could be mediated by astrocytes through the release of deleterious metabolic products or other substances. The lack of action of the astrocyte conditioned media on the viability of OLGc in the experiments in which we incubated OLGcs with the supernatant obtained from astrocyte cultures pretreated with CPZ, indicated that astrocytes did not appear to mediate OLGc damage by CPZ.

CPZ-induced demyelination is characterized by a robust microglia/macrophage response [9] and these cells are known to produce cytokines of the tumor necrosis factor (TNF) family, which are agents that have been implicated in the pathogenesis of CNS demyelinating diseases. Arnett et al. [26] showed that this cytokine was undetectable in the brain of untreated mice, but was upregulated during the course of CPZ-induced demyelination. The expression of TNFα was primarily detected in cells identified as

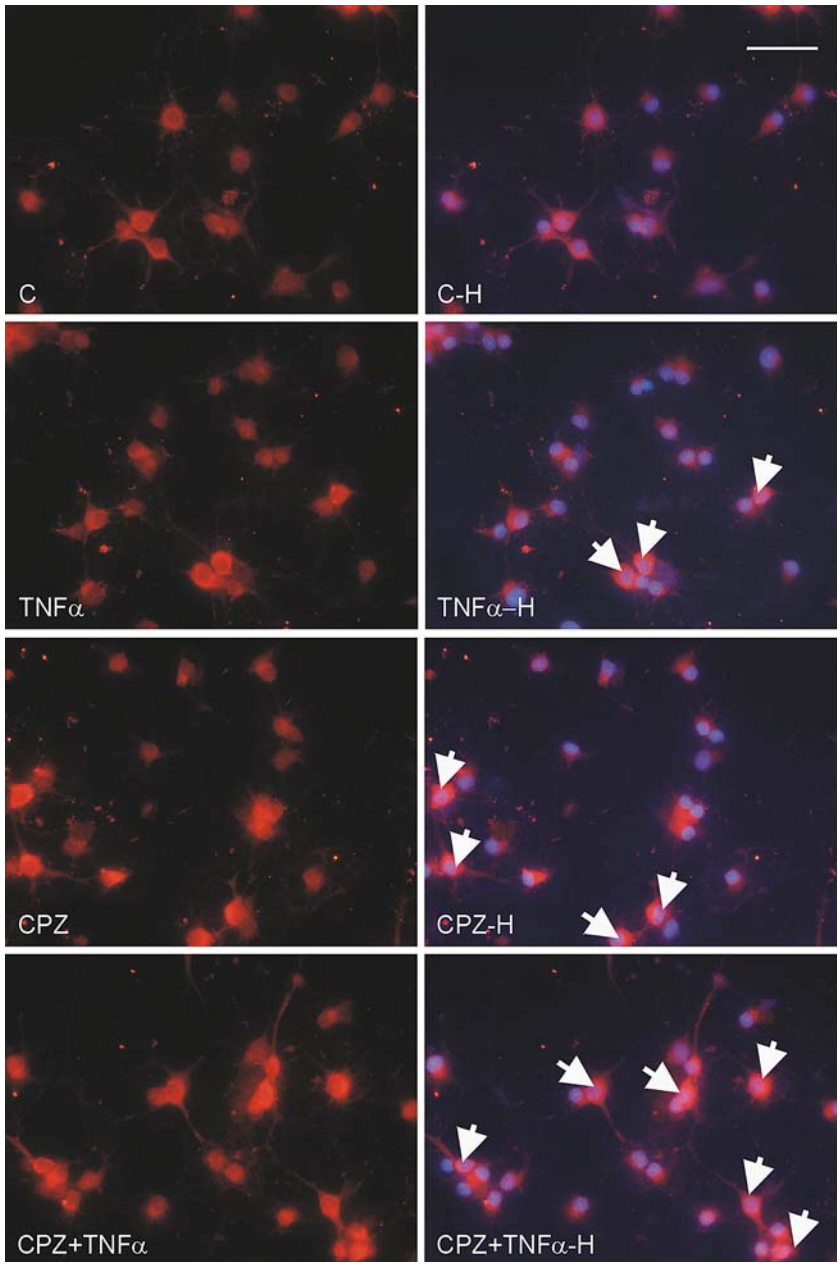

Fig. 5 Immunocytochemical analysis of NFκB (p65 subunit, red) and nuclear staining with Hoechst 33342 (blue) in OLGcs treated with CPZ and/or TNFα for 72 h. Arrows indicate NFκB reactivity in the nuclei. Scale bar corresponds to 8.2 μm. *Note*: For interpretation of the references to color in this figure legend, the reader is referred to the online version of this article

microglia and also in astroglial cells. TNFα, acting through TNFR1 is believed to mediate apoptosis, while when its action is exerted through TNFR2, it is known to enhance cell death or cell growth and proliferation [26].

The cells most heavily affected by neuroinflammation are oligodendrocytes. A large body of evidence suggests that cytokines, such as IFNγ and members of the TNF death ligand family (TNF/CD95L/NGF), are responsible for their degeneration [27–29]. Elevated levels of TNFα and IFNγ and their mRNAs in the blood and in the CSF often correlate with disease severity in MS [30–32].

TNF-family cytokines do not affect all types of glial cells uniformly. For example, TNFα stimulates astrocyte proliferation in vitro [33], proliferation of microglial cells co-cultured with astrocytes [34–36] and enhances microglia IL-1b-induced proliferation and IFNγ-induced nitric oxide production [37]. In contrast, in oligodendrocytes it has injurious effects such as inhibition of protein phosphorylation and process extension [38] and demyelination [39]. One way in which TNFα could differentially affect OLGcs is by altering their generation and/or neutralization of oxidant species. TNFα is known to disrupt the electron transport chain in mitochondria [40] initiating the

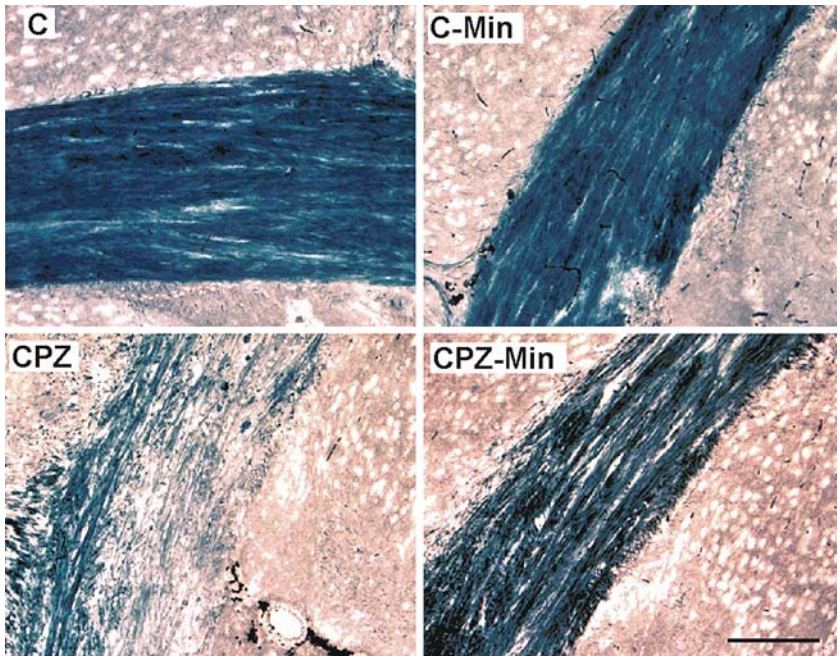

Fig. 6 Sudan Black staining of myelin in brain coronal sections obtained from mice intoxicated with CPZ, treated with minocycline and controls. Figure shows a section of the body of the corpus callosum. Abbreviations as in Fig. 9. Scale bars correspond to 150 μm. *Note*: For interpretation of the references to color in this figure legend, the reader is referred to the online version of this article

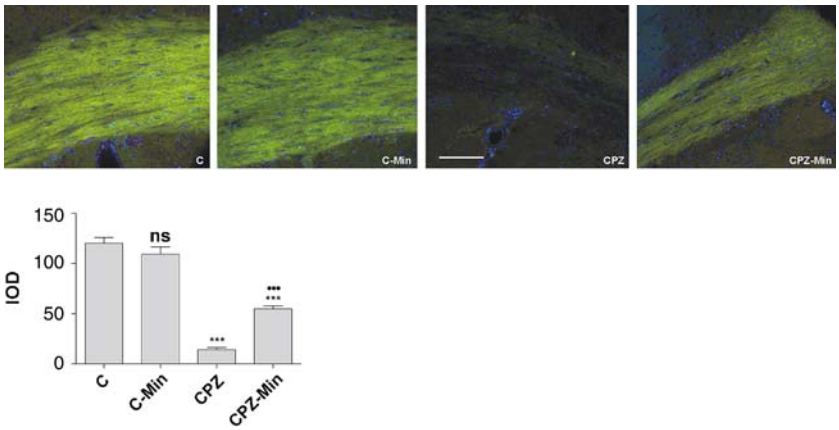

Fig. 7 Staining of myelin and cell nuclei using the BrainStain Imaging Kit (see Experimental Procedure) in brain coronal sections obtained from mice intoxicated with CPZ, treated with minocycline and controls. Figure shows a section of the body of the corpus callosum. Abbreviations as in Fig. 9. Scale bars correspond to 150 μm. Values are expressed as IOD and are the means ± SEM of three independent experiments (three replicates per experiment). ***$P < 0.001$ with reference to *C*. •••$P < 0.001$ with reference to *CPZ*. ns: nonsignificant. *Note*: For interpretation of the references to color in this figure legend, the reader is referred to the online version of this article

formation of superoxide anions, and mitochondria-derived oxidants are proposed to be instrumental in initiating apoptosis [41].

Rat microglia express both TNFR1 and TNFR2 in vitro, whereas OLGcs predominantly express TNFR1 [36]. The differential expression of TNF receptors and of the associated signaling pathways contributes, via differential oxidant species generation and/or neutralization, to the relative vulnerability of OLGcs to TNFα-induced injury. TNFα induced significantly stronger and more prolonged NFκB translocation, Mn SOD protein upregulation, and Mn SOD enzyme activity in microglia than in OLGcs.

The results show that CPZ does not significantly affect OLGc viability. However, when TNFα and/or IFNγ, at concentrations that have no harmful effects per se on cell viability, are added together with CPZ to the cultures, survival is significantly affected. These results suggest that these inflammatory cytokines could play a role in OLGc damage induced by CPZ.

Chew et al. [42] have demonstrated that under conditions of thyroid hormone-mediated oligodendro-

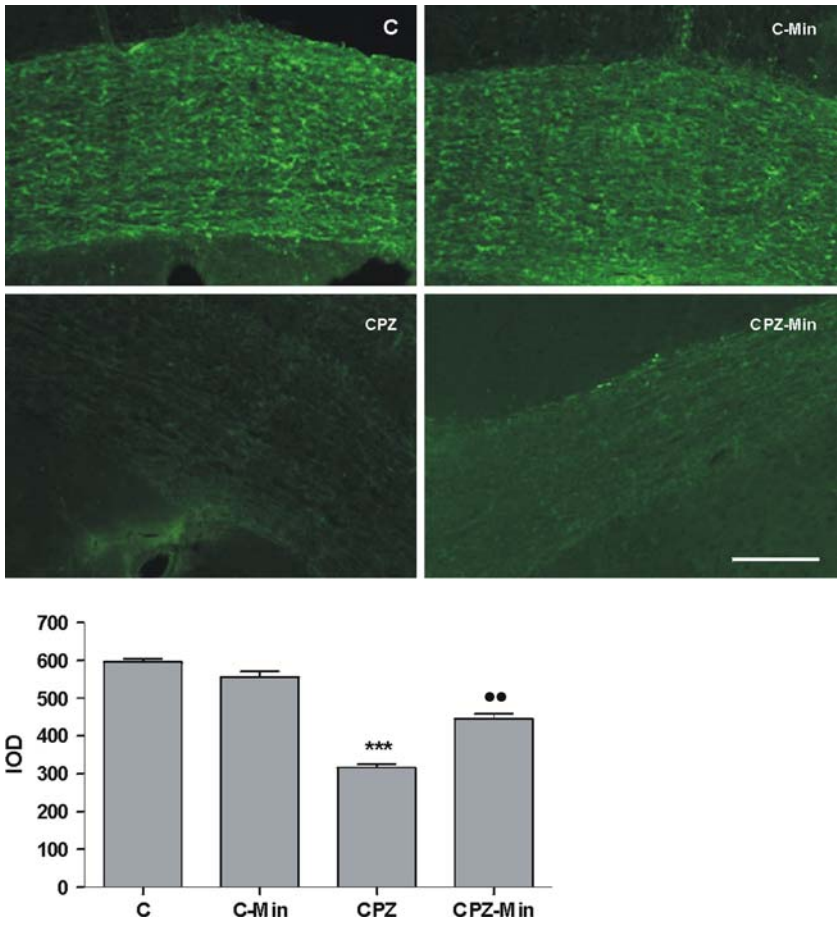

Fig. 8 MBP immunoreactivity in brain cryostat coronal sections obtained from mice intoxicated with CPZ, treated with minocycline and controls. Quantitative analysis of the sections was carried out using the Image Pro-Plus software and integration of the optical density (IOD) for MBP immunostaining was done as described in Fig. 9. Values are expressed as IOD and are the means ± SEM of three independent experiments (three replicates per experiment). ***$P < 0.001$ with reference to *C*. ••$P < 0.01$ with reference to *CPZ*. Scale bars correspond to 150 μm. *Note*: For interpretation of the references to color in this figure legend, the reader is referred to the online version of this article

cyte differentiation, IFNγ produced a dose-dependent apoptotic response in oligodendrocyte progenitors cells (OPCs). However, the lowest dose tested by these authors, (15 ng/ml), was nonapoptotic and inhibited cell cycle exit in differentiating OPCs. On the other hand, Arnett et al. [26] have demonstrated that TNFα promotes proliferation of OPCs through TNFR2. In our experiments, we work with low concentrations of IFNγ and/or TNFα, (between 0.1 ng/ml and 50 ng/ml). At these doses, we observe an apparent increase in cell viability. Alternatively this result could be due to an increase in cell proliferation, an explanation which is supported by the increase in the number of cells in S phase that we observe.

Flow cytometry studies showing that the percentage of cells in the S phase increases significantly when the cultures are treated with cytokines plus CPZ, indicating that the treated cells stop their maturation, support this conclusion and agree with previous results from Cammer [16]. In her studies of CPZ action on glial cultures, this investigator showed the presence of swollen or enlarged mitochondria in the treated cells, suggesting that these condition could compromise cell energy metabolism. Within this context, our results showing that in OLGc cultures treated with CPZ there is a marked decrease in the activities of complex I, II and III of the respiratory chain, indicate that CPZ disrupts mitochondrial function. These results were confirmed in our studies of mitochondria isolated from mice intoxicated with CPZ for 3–6 weeks.

Mitochondrial dysfunction is known to lead to the generation of increased amounts of oxidant species. We have observed a significant enhancement in the production of oxidants in OLGcs treated with either CPZ or with TNFα, which is higher when the cells are incubated with both compounds. The additive effects of both compounds suggest that they are probably exerted through independent pathways. Furthermore, our results showing a drop in the activity of all the complexes of the respiratory chain allow us to assume that the increased production of oxidant species is due to the mitochondrial dysfunction induced by the direct action of CPZ or of TNFα. However, this increased production of oxidants occurring when either substance is separately added to the cultures, does not seem to be sufficient to induce cell death. Contrariwise,

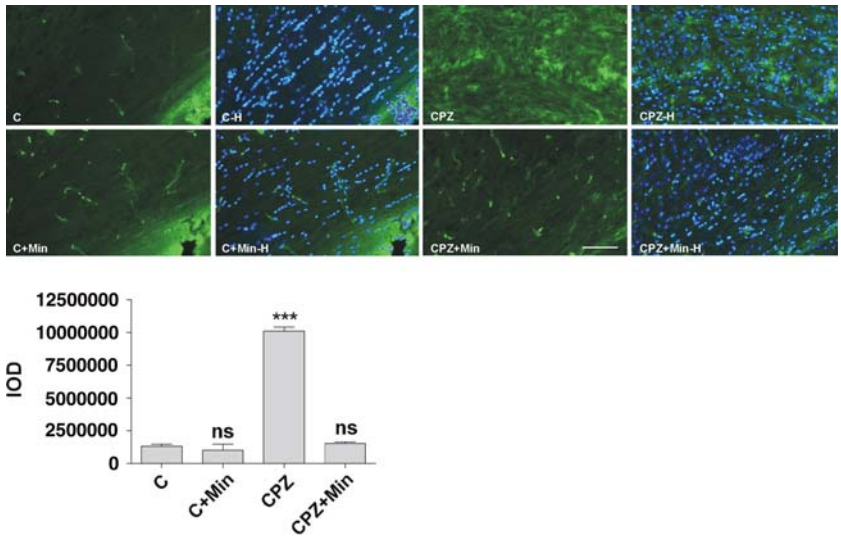

Fig. 9 Immunohistochemical analysis of microglial reactivity with CD11b antibody in brain coronal sections obtained from mice intoxicated with CPZ, treated with minocycline and controls. CD11b staining, green; Hoechst 33342 staining, (-**H**) blue. *C*: control. *C-Min*: minocycline-treated control. *CPZ*: cuprizone-treated animals. *CPZ-Min*: animals treated with CPZ and minocycline. Quantitative analysis of the sections was carried out using the Image Pro Plus software. Integration of the optical density (IOD) for CD11b immunostaining was measured for each experimental condition in five randomly selected fields of the body of the corpus callosum measuring 2.5 mm^2. Values are expressed as IOD and are the means ± SEM of three independent experiments (three replicates per experiment). ***$P < 0.001$. ns: nonsignificant. Scale bar corresponds to 150 μm. *Note*: For interpretation of the references to color in this figure legend, the reader is referred to the online version of this article

the addition of CPZ plus TNFα leads to cell death, which according to the results of caspase-3 activity that we have obtained, appears to be dependent on caspase-3 activation. Our observations agree with the results of Hisahara et al. [43] who observed activation of caspase-3 with TNFα treatment on OLGcs.

Signals derived from the activation of TNFR1 by TNFα binding, simultaneously induce an apoptotic cascade and a protective NFκB cascade, whereas TNFR2 signals primarily induce the protective NFκB cascade [44, 45]. Microglia expression of TNFR2 enables them to upregulate protective proteins that counteract the apoptotic signals transduced through TNFR1. Lacking TNFR2, OLGcs show less robust and less sustained NFκB nuclear translocation in response to TNFα. In agreement with these data, our results show an increase in the levels of NFκB with evidences of translocation of this factor to the nucleus in some of the cells treated with TNFα + CPZ, suggesting that the transcriptional activation of this factor occurs in these cells. Consequently, OLGcs thus treated do not appear to activate protective mechanisms and are acutely at risk of induced oxidative damage.

Minocycline, a second-generation tetracycline, may be an attractive candidate in the treatment of many neurodegenerative and trauma-induced CNS injuries attributable to both its anti-inflammatory and neuroprotective properties. The cellular and molecular basis for the neuroprotective effects of minocycline remains for the most part unknown. Collectively, the biological effects of minocycline include inhibition of microglial activation, reduction of the mRNA of both interleukin 1β (IL-1β) and inducible nitric oxide synthase [46], cyclooxygenase 2 expression, and prostaglandin E2 production [47]. Minocycline has also been shown to attenuate production of matrix metalloproteinases (MMPs) and to decrease T-lymphocyte transmigration [48, 49]. In addition, minocycline has been shown to inhibit caspase expression [50], cytochrome *c* release [51] and caspase-dependent and independent cell death [52].

Using minocycline-mediated inhibition of the microglia/macrophage activation, recent studies have shown that this drug provides protection against white matter injury induced by lipopolysaccharide, probably through inhibition of microglia activation [53] and protects oligodendrocyte development in the neonatal brain from hypoxia/ischemia injury [54]. Based on the hypothesis that the effect of CPZ on OLGcs could require the presence of cytokines secreted by microglia, one would predict that inhibition of microglia activation and its related inflammatory products with minocycline would lead to a decrease in the demyelinating effects of CPZ. Our results support this conclusion since minocycline administration to CPZ-treated mice markedly decreased microglia activation, as

shown by the diminished number of CD11b positive cells, and prevented demyelination, as demonstrated by morphological studies using myelin-specific staining and immunohistochemical techniques.

Based on the above-mentioned findings and contrary to the general belief indicating that activation of microglia in CPZ-induced demyelination takes place in order to remove the myelin debris that result from OLGc death, we suggest that these cells appear to have a much more active participation in the induction of OLGc death and demyelination, through the production and secretion of pro-inflammatory cytokines.

Acknowledgments Contract grant sponsor: Universidad de Buenos Aires B114 and Agencia Nacional de Promoción de Ciencia y Tecnología (PICT 12282). The authors wish to express their gratitude to Dra. Laura Pardo from FUNDALEU, for her help with the flow cytometry data.

References

1. Blakemore WF (1972) Observations on oligodendrocyte degeneration, the resolution of status spongiosus and remyelination in cuprizone intoxication in mice. J Neurocytol 1:413–426
2. Blakemore WF (1973) Remyelination of the superior cerebellar peduncle in the mouse following demyelination induced by feeding cuprizone. J Neurol Sci 20:73–83
3. Morell P, Barrett CV, Mason JL, Toews AD, Hostettler JD, Knapp GW, Matsushima GK (1998). Gene expression in brain during cuprizone induced demyelination and remyelination. Mol Cell Neurosci 12:220–227
4. Suzuki K, Kikkawa Y (1969) Status spongiosus of CNS and hepatic changes induced by cuprizone (biscyclohexanone oxalyldihydrazone). Am J Pathol 54:307–325
5. Hemm RD, Carlton WW, Welser JR (1971) Ultrastructural changes of cuprizone encephalopathy in mice. Toxicol Appl Pharmacol 18:869–882
6. Ludwin SK (1978) Central nervous system demyelination and remyelination in the mouse: an ultrastructural study of cuprizone toxicity. Lab Invest 39:597–612
7. Carleton WW (1967) Studies on the induction of hydrocephalus and spongy degeneration by cuprizone feeding and attempts to antidote the toxicity. Life Sci 6:11–19
8. Carey EM, Freeman NM (1983) Biochemical changes in cuprizone induced spongiform encephalopathy. I. Changes in the activities of 2',3'-cyclic nucleotide 3'-phosphohydrolase, oligodendroglial ceramide galactosyl transferase, and the hydrolysis of the alkenyl group of alkenyl, acyl-glycerophospholipids by plasmalogenase in different regions of the brain. Neurochem Res 6:1029–1044
9. Hiremath MM, Saito Y, Knapp GW, Ting JP, Suzuki K, Matsushima GK (1998) Microglial/macrophage accumulation during cuprizone-induced demyelination in C57BL/6 mice. J Neuroimmunol 92:38–49
10. Shohami E, Ginis I, Hallenbeck JM (1999) Dual role of tumor necrosis factor alpha in brain injury. Cytokine Growth Factor Rev 10:119–130
11. Liu C, Li Wan Po A, Blumhardt LD (1998) ''Summary measure'' statistic for assessing the outcome of treatment trials in relapsing-remitting multiple sclerosis. J Neurol Neurosurg Psychiatry 64:726–729
12. Kassiotis G, Kollias G (2001) TNF and receptors in organ-specific autoimmune disease: multi-layered functioning mirrored in animal models. J Clin Invest 107:1507–1508
13. Buntinx M, Moreels M, Vandenabeele F, Lambrichts I, Raus J, Steels P, Stinissen P, Ameloot M (2004) Cytokine-induced cell death in human oligodendroglial cell lines: I. Synergistic effects of IFN-gamma and TNF-alpha on apoptosis. J Neurosci Res 76:834–845
14. Cammer W (2002) Protection of cultured oligodendrocytes against tumor necrosis factor-alpha by the antioxidants coenzymes Q (10) and N-acetyl cysteine. Brain Res Bull 58:587–592
15. Jurewicz A, Matysiak M, Tybor K, Selmaj K (2003) TNF-induced death of adult human oligodendrocytes is mediated by c-jun NH2-terminal kinase-3 Brain 126:1358–1370
16. Cammer W (1999) The neurotoxicant cuprizone retards the differentiation of oligodendrocytes in vitro. J Neurol Sci 168:116–120
17. McCarthy KD, de Vellis J (1980) Preparation of separate astroglial and oligodendroglial cell cultures from rat cerebral tissue. J Cell Biol 85:890–902
18. Casaccia-Bonnefil P, Aibel L, Chao MV (1996) Central glial and neuronal populations display differential sensitivity to ceramide-dependent cell death. J Neurosci Res 43:382–389
19. Mosmann T (1983) Rapid colorimetric assay for cellular growth and survival: application to proliferation and cytotoxicity assays. J Immunol Methods 65:55–63
20. Oberhammer F, Fritsch G, Schmied M, Pavelka M, Printz D, Purchio T, Lassmann H, Schulte-Hermann R (1993) Condensation of the chromatin at the membrane of an apoptotic nucleus is not associated with activation of an endonuclease. J Cell Sci 104:317–326
21. De Robertis EDF, Pellegrino de Iraldi A, Rodriguez de Lorez Arnaiz G, Salganicoff L (1962) Cholinergic and non-cholinergic nerve ending in rat brain. J Neurochem 9:23–35
22. Morais Cardoso S, Pereira C, Resende Oliveira C (1999) Mitochondrial function is differentially affected upon oxidative stress. Free Radic Biol Med 26:3–13
23. Matsushima GK, Morell P (2001) The neurotoxicant, cuprizone, as a model to study demyelination and remyelination in the central nervous system. Brain Pathol 11:107–116
24. Giuliani F, Fu SA, Metz LM, Yong VW (2005) Effective combination of minocycline and interferon-beta in a model of multiple sclerosis. J Neuroimmunol 165:83–91
25. Adamo AM, Paez PM, Escobar Cabrera OE, Wolfson M, Franco PG, Pasquini JM, Soto EF (2006) Remyelination after cuprizone-induced demyelination in the rat is stimulated by apotransferrin. Exp Neurol 198:519–529
26. Arnett H, Mason J, Marino M, Suzuki K, Matsushima GK, Ting JP (2001) TNF alpha promotes proliferation of oligodendrocyte progenitors and remyelination. Nat Neurosci 4:1116–1122
27. Selmaj K, Raine CS, Cannella B, Brosnan CF (1991) Identification of lymphotoxin and tumor necrosis factor in multiple sclerosis lesions. J Clin Invest 87:949–954
28. Vartanian T, Li Y, Zhao M, Stefansson K (1995) Interferon-gamma-induced oligodendrocyte cell death: implications for the pathogenesis of multiple sclerosis. Mol Med 1:732–743

29. D'Souza SD, Bonetti B, Balasingam V, Cashman NR, Barker PA, Troutt AB, Raine CS, Antel JP (1996) Multiple sclerosis: Fas signaling in oligodendrocyte cell death. J Exp Med 184:2361–2370
30. Martino G, Consiglio A, Franciotta DM, Corti A, Filippi M, Vandenbroeck K, Sciacca FL, Comi G, Grimaldi LM (1997) Tumor necrosis factor alpha and its receptors in relapsing-remitting multiple sclerosis. J Neurol Sci 152:51–61
31. Debruyne J, Philippe J, Dereuck J, Willems A, Leroux-Roels G (1998) Relapse markers in multiple sclerosis: are in vitro cytokine production changes reflected by circulatory T-cell phenotype alterations? Mult Scler 4:193–197
32. Vandevyver C, Motmans K, Stinissen P, Zhang J, Raus J (1998) Cytokine mRNA profile of myelin basic protein reactive T-Cell clones in patients with multiple sclerosis. Autoimmunity 28:77–89
33. Merrill JE (1991) Effects of interleukin-1 and tumor necrosis factor-alpha on astrocytes, microglia, oligodendrocytes, and glial precursors in vitro. Dev Neurosci 13:130–137
34. Giulian D, Ingeman JE (1988) Colony-stimulating factors as promoters of ameboid microglia. J Neurosci 8:4707–4717
35. Théry C, Mallat M (1993) Influence of interleukin-1 and tumor necrosis factor alpha on the growth of microglial cells in primary cultures of mouse cerebral cortex: involvement of colony-stimulating factor 1. Neurosci Lett 150:195–199
36. Dopp JM, Mackenzie-Graham A, Otero GC, Merrill JE (1997) Differential expression, cytokine modulation, and specific functions of type-1 and type-2 tumor necrosis factor receptors in rat glia. J Neuroimmunol 75:104–112
37. Merrill JE, Ignarro LJ, Sherman MP, Melinek J, Lane TE (1993) Microglial cell cytotoxicity of oligodendrocytes is mediated through nitric oxide. J Immunol 151:2132–2141
38. Soliven B, Szuchet S (1995) Signal transduction pathways in oligodendrocytes: role of tumor necrosis factor-alpha. Int J Dev Neurosci 13:351–367
39. Selmaj KW, Raine CS (1988) Tumor necrosis factor mediates myelin and oligodendrocyte damage in vitro. Ann Neurol 23:339–346
40. Goossens V, Grooten J, De Vos K, Fiers W (1995) Direct evidence for tumor necrosis factor-induced mitochondrial reactive oxygen intermediates and their involvement in cytotoxicity. Proc Natl Acad Sci USA 92:8115–8119
41. Green DR, Reed JC (1998) Mitochondria and apoptosis. Science 281:1309–1312
42. Chew LJ, King WC, Kennedy A, Gallo V (2005) Interferon-gamma inhibits cell cycle exit in differentiating oligodendrocyte progenitor cells. Glia 52:127–143
43. Hisahara S, Shoji S, Okano H, Miura M (1997) ICE/CED-3 family executes oligodendrocyte apoptosis by tumor necrosis factor. J Neurochem 69:10–20
44. Hsu H, Shu H, Pan M, Goeddel D (1996) TRADDTRAF2 and TRADD-FADD interactions define two distinct TNF receptor 1 signal transduction pathways. Cell 84:299–308
45. Rothe M, Wong S, Henzel W, Goeddel D (1994) A novel family of putative signal transducers associated with the cytoplasmic domain of the 75 kDa tumor necrosis factor receptor. Cell 78:681–692
46. Yrjanheikki J, Keinanen R, Pellikka M, Hokfelt T, Koistinaho J (1998) Tetracyclines inhibit microglial activation and are neuroprotective in global brain ischemia. Proc Natl Acad Sci USA 95:15769–15774
47. Yrjanheikki J, Tikka T, Keinanen R, Goldsteins G, Chan PH, Koistinaho J (1999) A tetracycline derivative, minocycline, reduces inflammation and protects against focal cerebral ischemia with a wide therapeutic window. Proc Natl Acad Sci USA 96:13496–13500
48. Brundula V, Rewcastle NB, Metz LM, Bernard CC, Yong VW (2002) Targeting leukocyte MMPs and transmigration: minocycline as a potential therapy for multiple sclerosis. Brain 125:1297–1308
49. Power C, Henry S, Del Bigio MR, Larsen PH, Corbett D, Imai Y, Yong VW, Peeling J (2003) Intracerebral hemorrhage induces macrophage activation and matrix metalloproteinases. Ann Neurol 53:731–742
50. Chen M, Ona VO, Li M, Ferrante RJ, Fink KB, Zhu S, Bian J, Guo L, Farrell LA, Hersch SM, Hobbs W, Vonsattel JP, Cha JH, Friedlander RM (2000) Minocycline inhibits caspase-1 and caspase-3 expression and delays mortality in a transgenic mouse model of Huntington disease. Nat Med 6:797–801
51. Zhu S, Stavrovskaya IG, Drozda M, Kim BYS, Ona V, Li M, Sarang S, Liu AS, Hartley DM, Wu DC, Gullans S, Ferrante RJ, Przedborski S, Kristal BS, Friedlander RM (2002) Minocycline inhibits cytochrome *c* release and delays progression of amyotrophic lateral sclerosis in mice. Nature 417:74–78
52. Wang X, Zhu S, Drozda M, Zhang W, Stavrovskaya IG, Cattaneo E, Ferrante RJ, Kristal BS, Friedlander RM (2003) Minocycline inhibits caspase-independent and -dependent mitochondrial cell death pathways in models of Huntington's disease. Proc Natl Acad Sci USA 100:10483–10487
53. Fan LW, Pang Y, Lin S, Tien LT, Ma T, Rhodes PG, Cai Z (2005) Minocycline reduces lipopolysaccharide induced neurological dysfunctions and brain injury in the neonatal rat. J Neurosci Res 82:71–82
54. Cai Z, Lin S, Fan LW Pang Y, Rhodes PG (2006) Minocycline alleviates hypoxic-ischemic injury to developing oligodendrocytes in the neonatal rat brain. Neuroscience 137:425–435